Supporting Information for

Dual Role of hBN as an Artificial Solid-Electrolyte Interface Layer for Safe Zinc Metal Anodes

Hoilun Wong[1#], Tsz Wing Tang[1#], Haoliang Chen[2], Mengyang Xu[1], Jun Wang[1], Yuting Cai[1], William A. Goddard III[3*], Zhengtang Luo[1,4*]

[1] *Department of Chemical and Biological Engineering and William Mong Institute of Nano Science and Technology, Hong Kong University of Science and Technology, Clear Water Bay, Kowloon, Hong Kong*

[2] *School of Materials Science and Engineering, and Guangdong Provincial Key Laboratory of Advanced Energy Storage Materials, South China University of Technology, Guangzhou, Guangdong, 510640, PR China*

[3] *Materials and Process Simulation Center (MSC), California Institute of Technology, MC 139-74, Pasadena, CA 91125, USA*

[4] *Hong Kong University of Science and Technology-Shenzhen Research Institute, No. 9 Yuexing first RD, Hi-Tech Park, Nanshan, Shenzhen 518057, China*

E-mail: wag@caltech.edu; ORCID: 0000-0003-0097-5716
E-mail: keztluo@ust.hk

Experimental Section

Computational method: The DFT calculations with the spin-polarization were performed using the Vienna ab initio simulation package (VASP) code[1-3]. vdW-DF2 functionals were utilized to describe van der Waals (vdW) interactions, while general gradient approximation (GGA) exchange correlation functionals of Perdew-Burke-Ernzerhof (PBE) was employed to depict the exchange correlation. For the ion-electron interactions, it is described by projector augment wave (PAW) pseudopotential.[4, 5] The cut-off energy was set to 500 eV and the K-points were set to 5 × 5 × 1 for both structure relaxation and energy calculation. For the structure relaxation, the convergence criteria for electron self-consistent loop and the Hellman–Feynman forces were 10^{-6} and 0.02 eV $Å^{-1}$, respectively. Throughout the whole calculation, a Gaussian smearing was set to be 0.05 eV. To study the adsorption of Zn on hBN and Zn (002), the supercell of 5 × 5 hBN (12.56 × 12.56 Å) and 3 × 3 Zn (002) (10.47 × 10.47) were built with vacuum space in the z-axis of 20 Å to ensure the intermolecular interactions. The adsorption energy (E_{ads}) was calculated by the following equation (1):

$$E_{ads} = E_{total} - (E_{substrate} + E_{Zn}) \quad (1)$$

Where E_{total} is the total energy of system with Zn adsorbed on substrate; $E_{substrate}$ refers to the energy of the substrate; and E_{Zn} is the energy of the single Zn atom. The 3D model structures were visualized by VESTA software.[6]

Preparation of hBN film: The Cu foil (Alfa Aesar, #13382) was chemically washed in acetic acid for 10 minutes and rinsed with DI water before hBN samples were grown on it. The dried Cu foil was then placed on a quartz plate and loaded into the middle of a tube furnace. The B and N precursor, ammonia borane (AB), was positioned upstream 32cm from the Cu foil and heated by a heating coil. The system was purged with 250 sccm argon for 15 minutes, ramped up to 1045°C over 30 minutes, and annealed with a mixed gas of 250 sccm argon and 25 sccm hydrogen for 45 minutes. The hBN growth process began by heating up the heating coil to 90°C and continued for a certain duration to produce monolayered grains (20 minutes) or continuous films (60 minutes). Finally, the growth was stopped by turning off the furnace and rapidly cooling down to room temperature with argon flow.

Preparation of hBN/Zn: The as-grown hBN was transferred to a targeted substrate using the PMMA-assisted bubble transfer method. The hBN/Cu was first cut into the desired size and spin-coated with PMMA (500 rpm for 10 seconds, followed by 3000 rpm for 50 seconds). During bubble transfer, the PMMA/hBN worked as the cathode with a Pt anode in 1M sodium hydroxide solution. The separated PMMA/hBN was then transferred and floated onto DI water to remove any remaining ions for 20 minutes. Next, the PMMA/hBN was scooped up with the Zn substrate and dried in an oven at 60°C. Finally, the PMMA was removed by immersing the sample in acetone overnight.

Preparation of Al_xVOH: All chemicals with analytical grade were purchased from Sigma-Aldrich and deionized (DI) water was used throughout the whole work. Typically, 2 mmol vanadium pentoxide was firstly dispersed in 80 mL DI water. Then, 4 mL hydrogen peroxide was added into the above suspension. After stirring for 10 min, 0.12 mmol $Al_2(SO_4)_3 \cdot 18H_2O$ was added and then the solution was transferred into a 100 mL Teflon-lined autoclave and kept at 180 °C for 12 h. After centrifuging several times with water and alcohol, the Al_xVOH sample were collected. Finally, the resulting product was further dried at 120 °C in a vacuum oven overnight.

Materials characterization: The morphology of the as-grown hBN was observed using an optical microscope (LEICA DMLM), Transmission Electron Microscopy (TEM, JEOL 2010F) and Scanning electron microscope (SEM, Super 40, Zeiss) with the Energy dispersive analysis (EDS, XFlash Detector 5010, Bruker equipment). The structure was characterized by Raman spectroscopy (Renishaw Raman RM3000scope) with a 514 nm laser and X-ray photoelectron spectroscopy (XPS, Thermal Fisher, ESCALAB 250Xi). The thickness of the hBN crystals was measured using atomic force microscopy (AFM, Bruker Innova) with a 670nm laser diode (Class b).

Electrochemical measurement: The electrochemical measurements of as-prepared Al_xVOH were investigated via assembling 2025-type coin cells in the air. The working electrode slice was prepared by mixing Al_xVOH, carbon nanotubes and polyvinylidene fluoride (the quality ratio is 7:2:1) in N-methyl pyrrolidone solvent, and then the slurry was adequately grinded, coated on titanium foil (0.03 mm thickness) and dried in a vacuum oven at 60 °C for 12 h. Zn metal, glass fiber membrane (Whatman GF/D) and 2 M $ZnSO_4$ aqueous solution used as the anode, separator, and electrolyte, respectively. The traditional galvanostatic discharge-charge (GDC) measurements were investigated on Neware system within the cutoff voltage ranges of 0.2-1.6 V. Cyclic voltammograms curves was collected from the Gamry-Reference 1000 electrochemical workstation.

The calculation of relative texture coefficients ($^{RTC}{}_{(hkl)}$): The RTC of the crystal planes of (*hkl*) was calculated as follow:

$$RTC_{(hkl)}(\%) = \frac{I_{(hkl)}/I^{std}_{(hkl)}}{\sum_{1}^{n} I_{(hkl)}/I^{std}_{(hkl)}} \times 100\% \quad (1)$$

where $I_{(hkl)}$ and $I^{std}_{(hkl)}$ are the intensities of (hkl) crystal plane in the analyzed sample and standard Zn, respectively. *n* is the number of samples.

The calculation of lattice mismatch(f):

$$|f| = \frac{a_{Zn} - a_{hBN}}{a_{hBN}} \times 100\% \quad (2)$$

where a_{Zn} and a_{hBN} are the lattice constants of Zn (002) and hBN, respectively.

The calculation of surface energy (γ):

$$\gamma = \frac{1}{2A}(E_{surface} - nE_{bulk}) \quad (3)$$

where $E_{surface}$ the total energy of relaxed surface, E_{bulk} is the total energy of bulk unit cell, *A* is the area of the determining surface, *n* is number of repeating bulk unit cell in surface model.

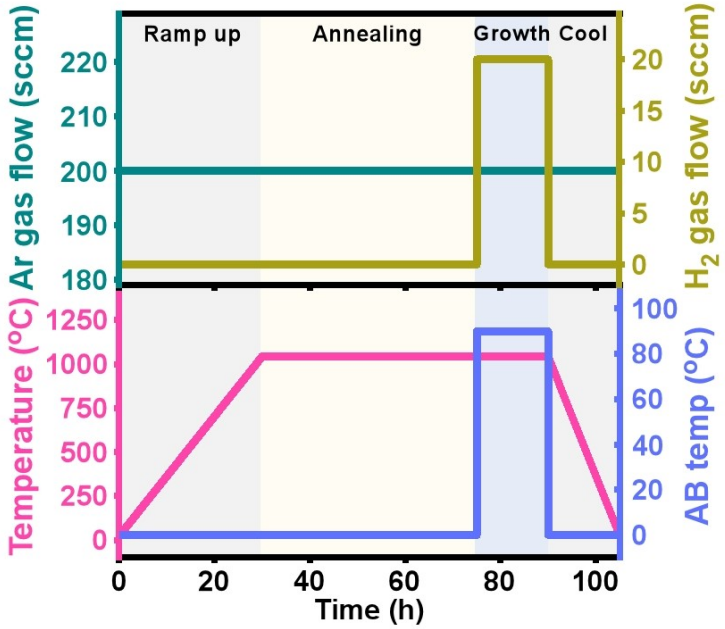

Figure S1. Growth conditions of hBN preparation in temperature of the furnace heating, precursor (AB) temperature, Ar and H_2 gas flow.

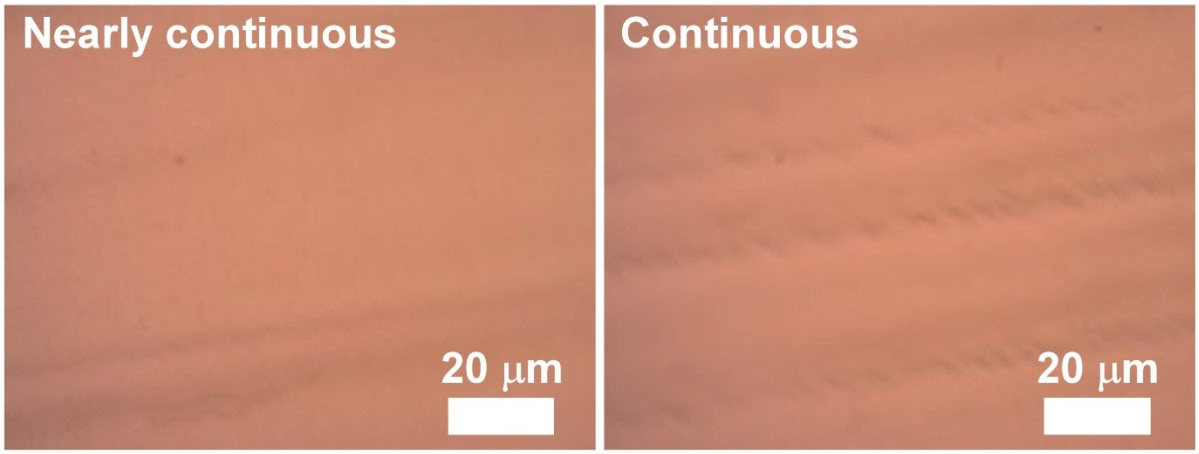

Figure S2. Optical microscopy of nearly continuous and continuous growth of hBN film on Cu substrate.

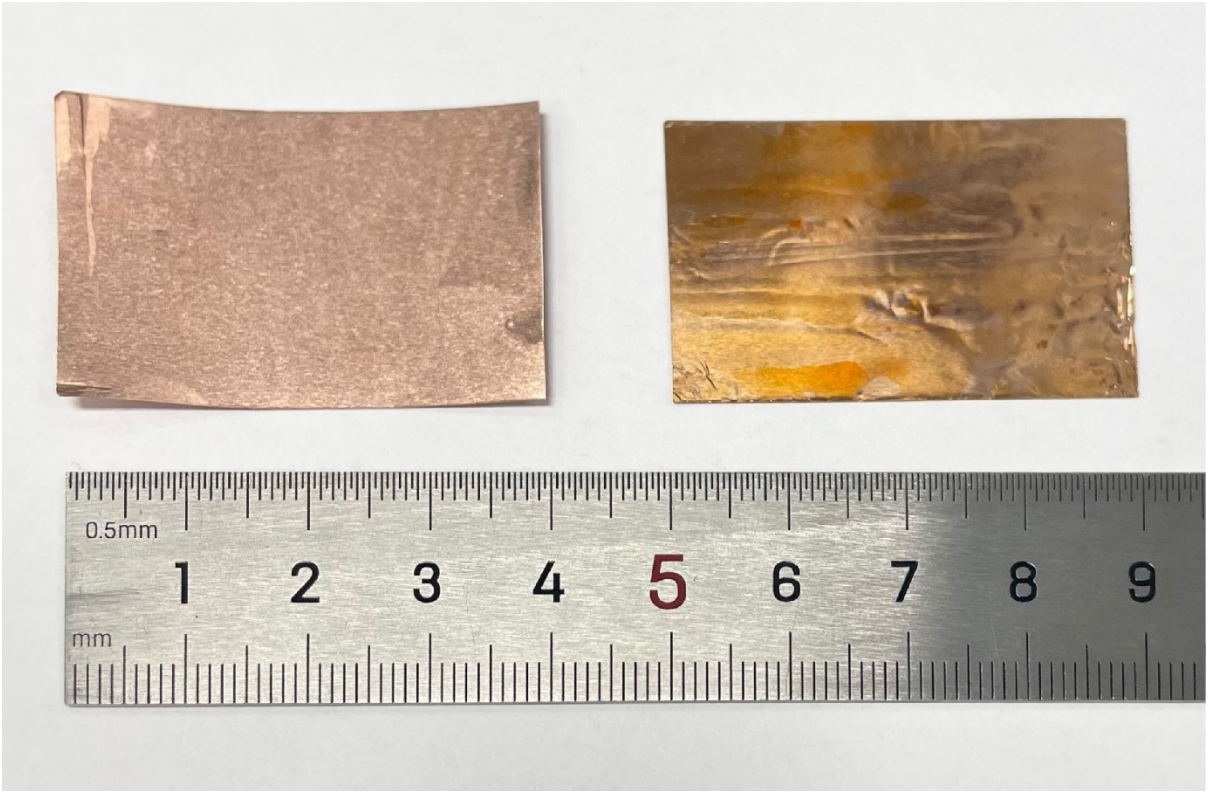

Figure S3. Optical image of Cu foils exposed to O_2 under annealing. Cu foils covered with fully grown hBN (hBN/Cu) on the left and without hBN on the right after annealing in air (200°C, 5 min).

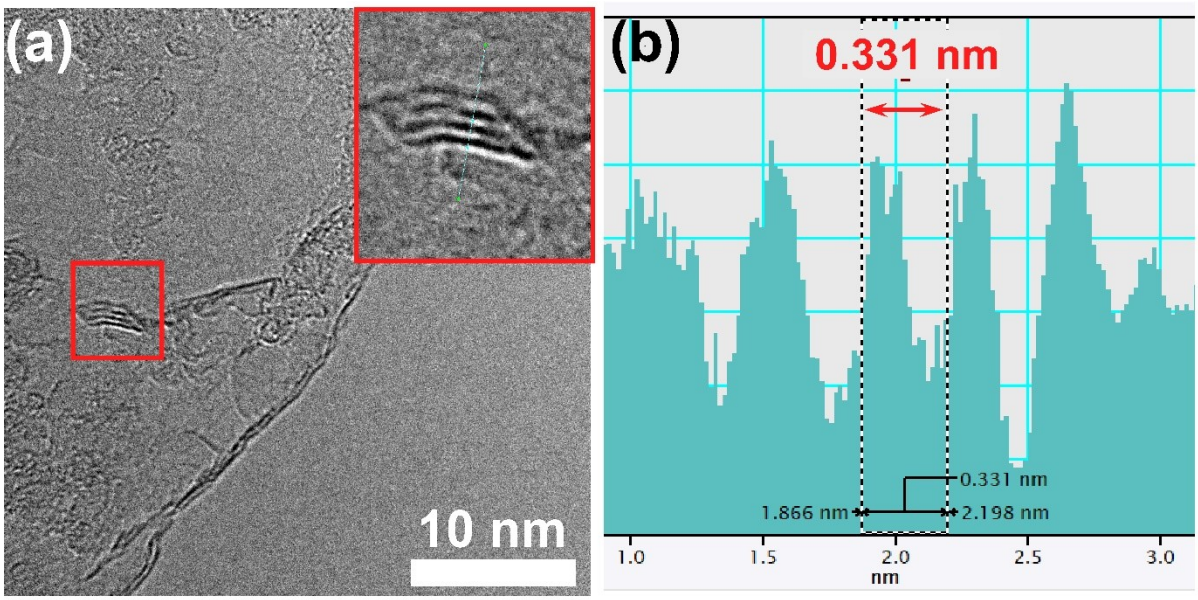

Figure S4. Transmission Electron Microscopy (TEM) characterizations of multilayer continuously grown hBN. (a) High magnification of TEM image of hBN with enlarged inset of the folded edge. (b) Measurement of the interlayer distance of hBN is 0.331 nm.

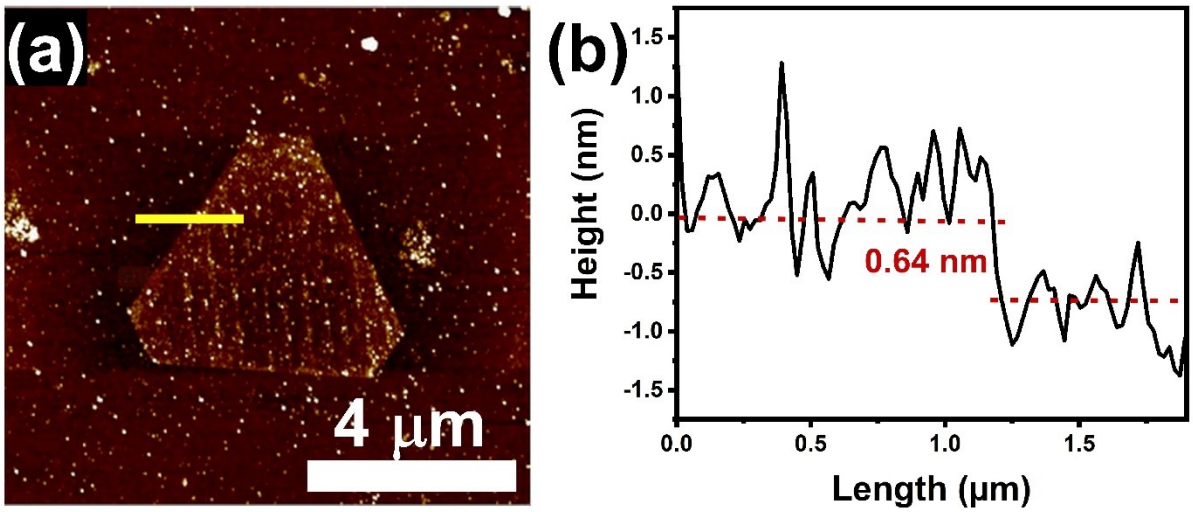

Figure S5. Atomic force microscopy (AFM) characterizations of hBN. (a) AFM image of transferred hBN domains on silicon wafer with the (b) height profile, showing the 0.64 nm film thickness.

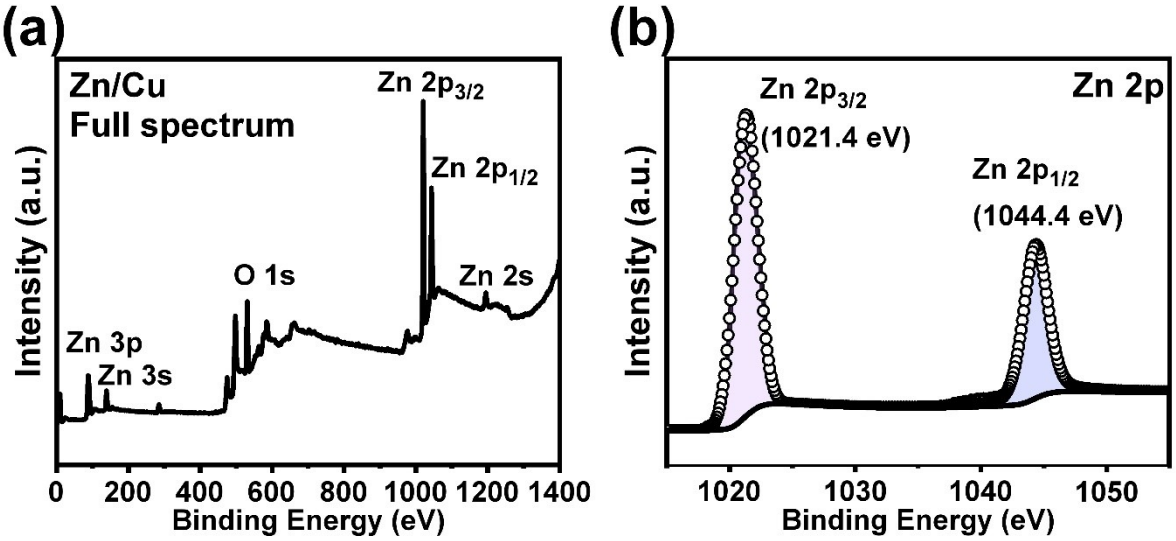

Figure S6. XPS results of deposited Zn on hBN/Cu. (a) Full XPS spectrum and (b) high resolution XPS spectrum of Zn 2p.

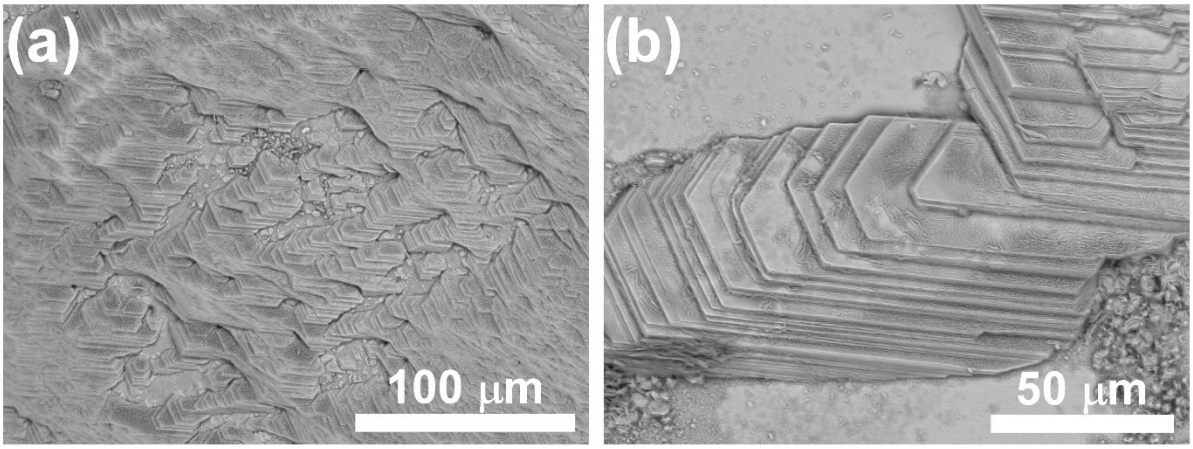

Figure S7. SEM characterization of Zn deposits on Cu surface. (a) low and (b) high magnification of SEM images showing hexagonal shaped and highly compact Zn electrodeposition.

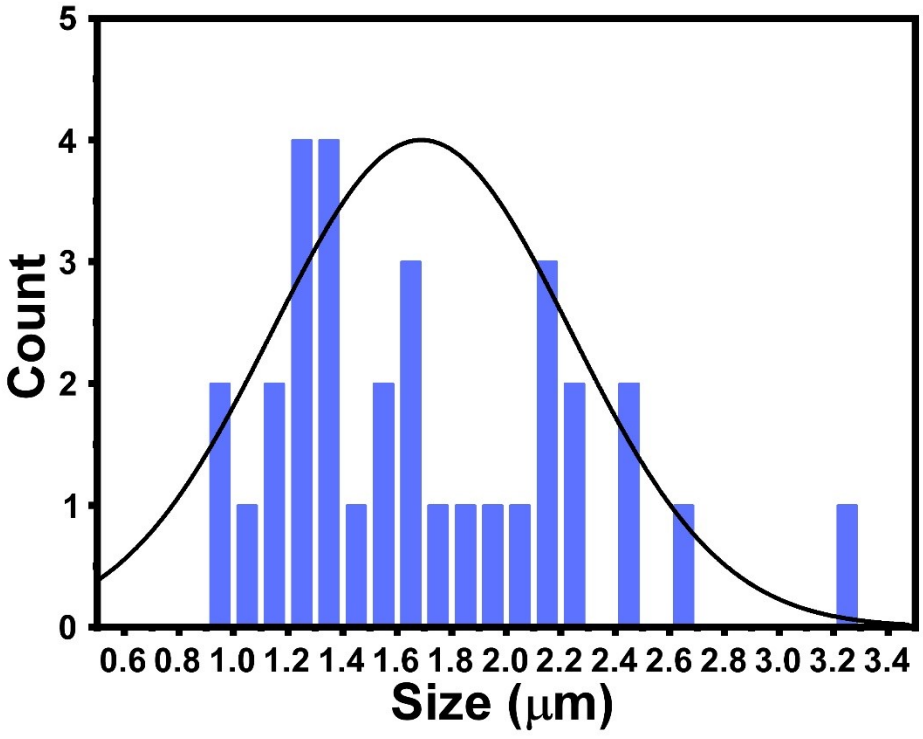

Figure S8. Size distribution of deposited Zn on hBN/Cu. The result shows that the average size of deposited Zn is 1.7 μm from the range of 1.0-3.2 μm.

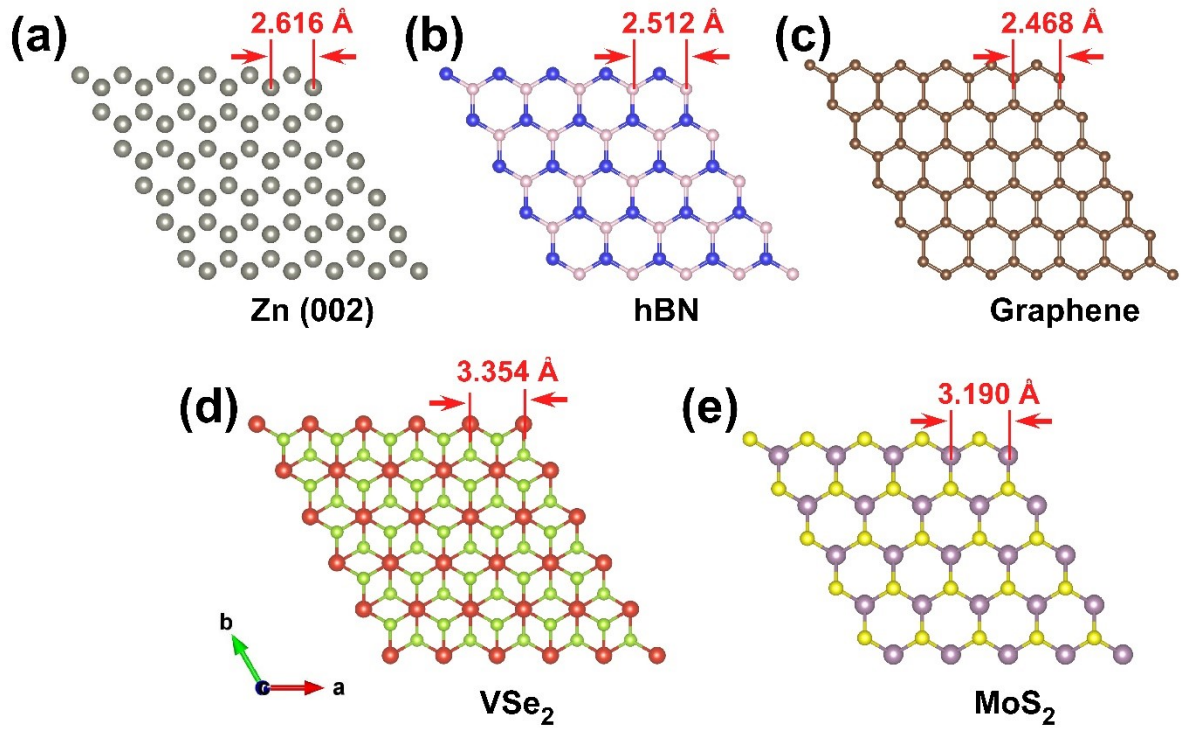

Figure S9. Lattice arrangement of (a) Zn (002), (b) hBN, (c) graphene, (d) VSe_2 and (e) MoS_2. The lattice mismatch is calculated in the formula of $\frac{a_{Zn} - a_{hBN}}{a_{hBN}} \times 100\%$.

Table S1. Lattice mismatch between the Zn (002) and the corresponding surfaces of hBN, graphene, MoS_2 and VSe_2.

Substrate	Lattice mismatch (%)
hBN	4.12
Graphene	6.01
MoS_2	18.00
VSe_2	22.00

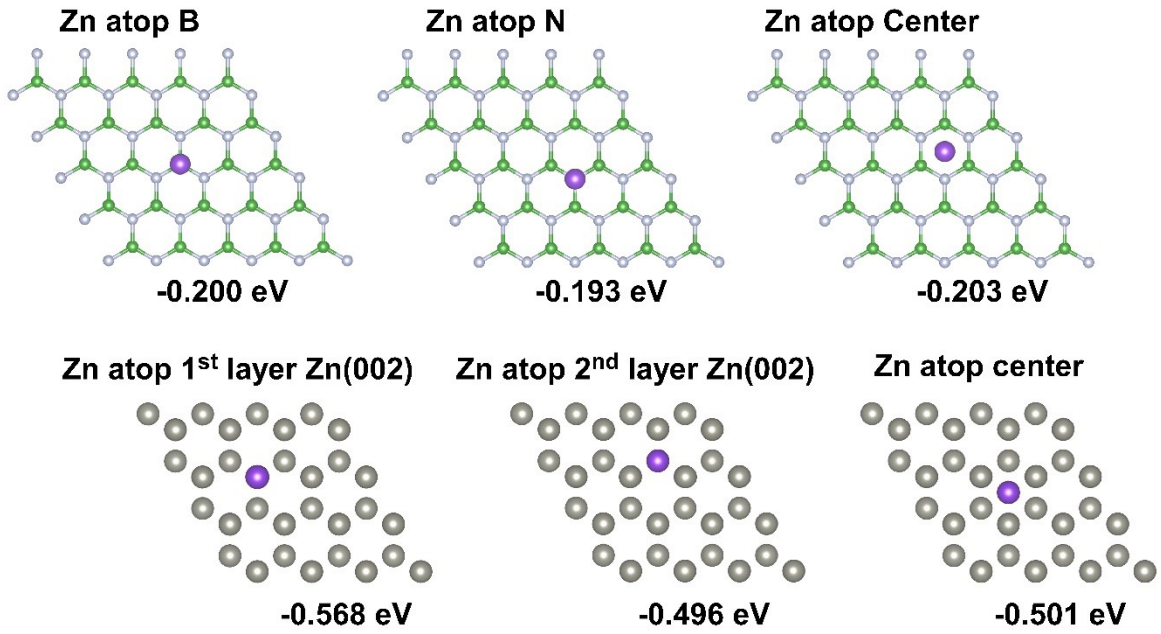

Figure S10. Zn atom binding energy at different adsorption sites on hBN and Zn (002) surfaces. (Zn in purple and silver colors represents the adsorbed Zn atom and Zn atom in Zn (002) slab)

Table S2. Parameters for calculating the surface energies of hBN and Zn (002).

Substrate	$E_{surface}$ (eV)	E_{bulk} (eV)	A (Å^2)	n
hBN	-159.77	-35.62	56.85	4.5
Zn (002)	-88.49	-5.96	109.56	16

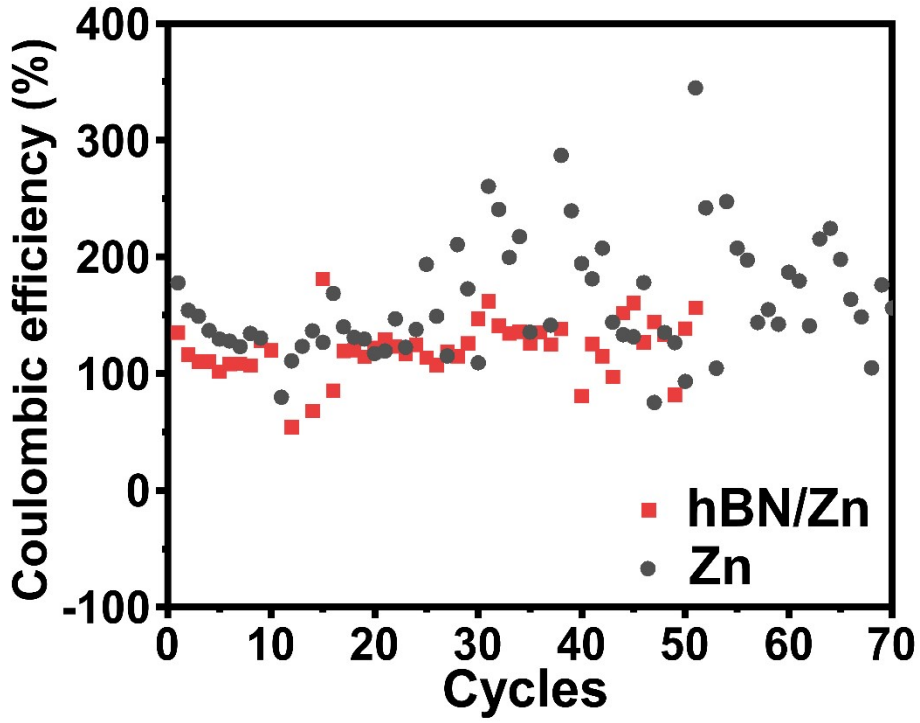

Figure S11. Coulombic efficiency of hBN/Zn and Zn electrodes.

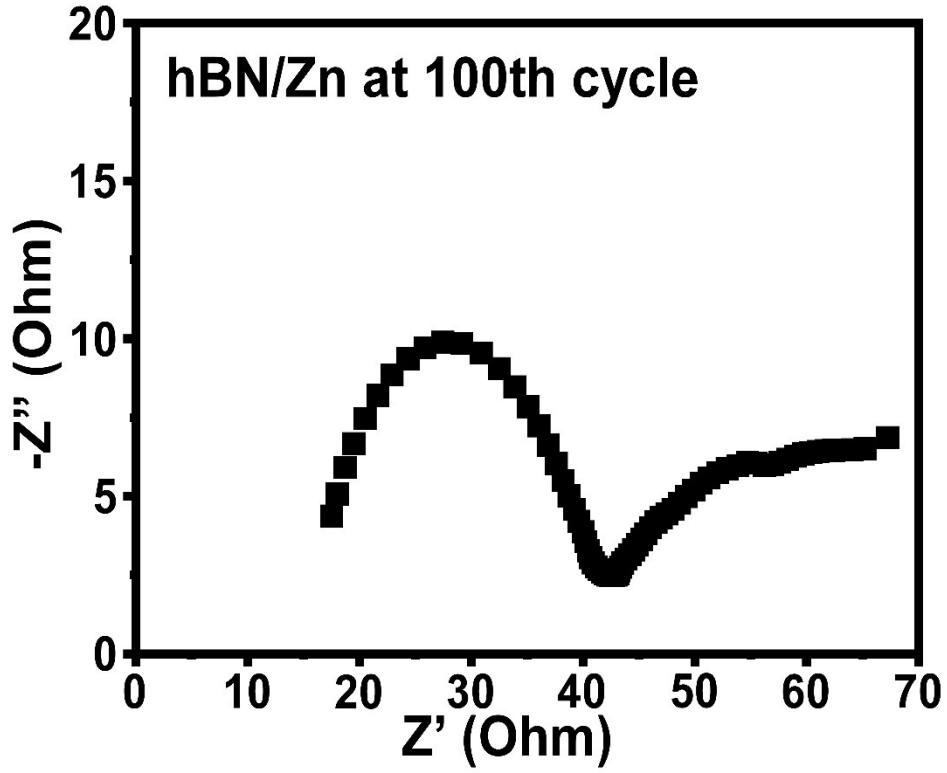

Figure S12. EIS results of hBN/Zn electrodes after 100 cycles.

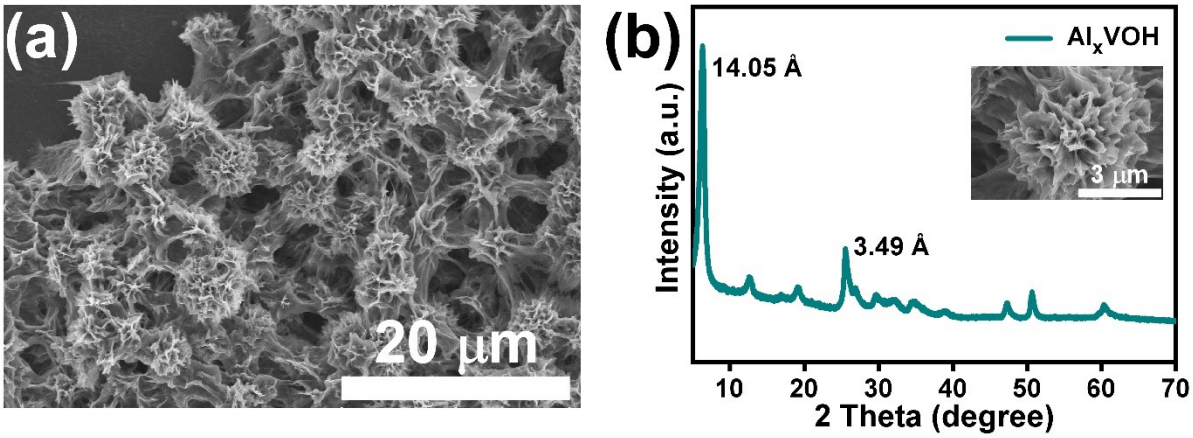

Figure S13. Morphology and structure characterizations of cathode material for full cell testing. (a) SEM image and (b) XRD results of Al_xVOH.

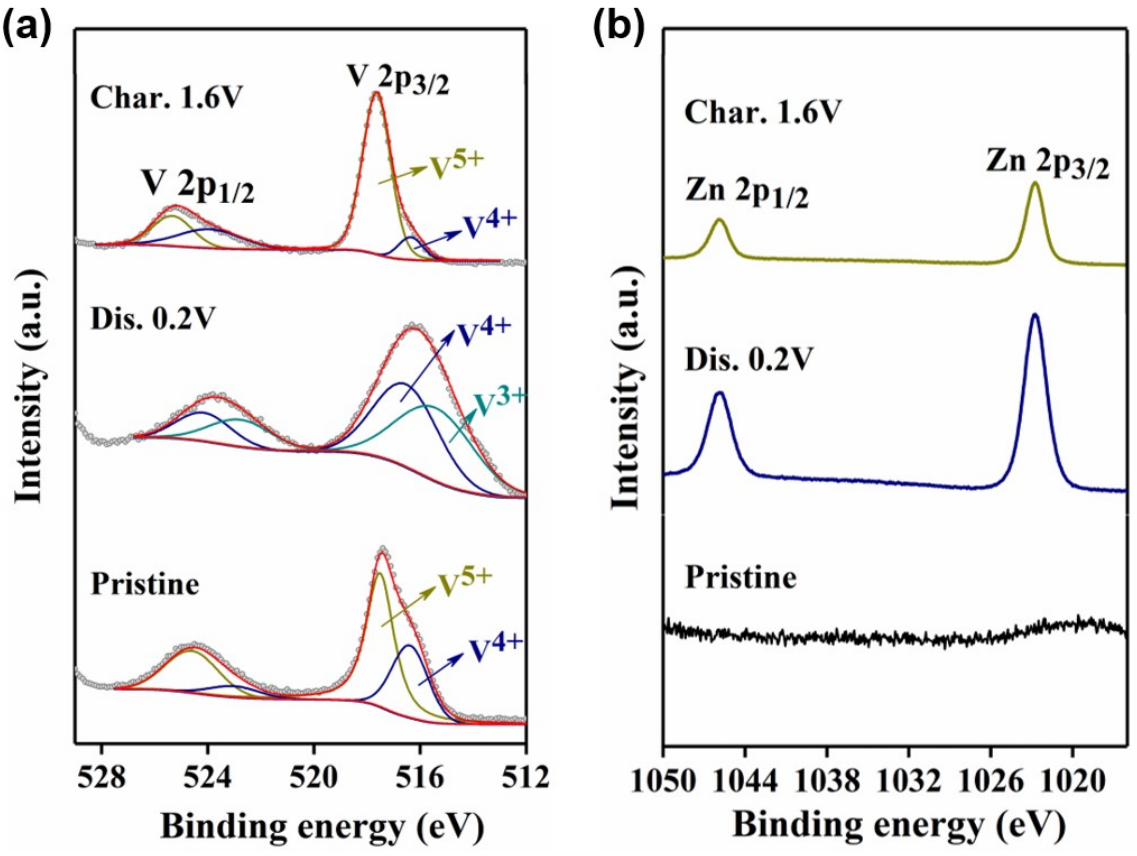

Figure S14. Ex-situ XPS characterization of Al_xVOH cathode. (a) V 2p and (b) Zn 2p spectrum.

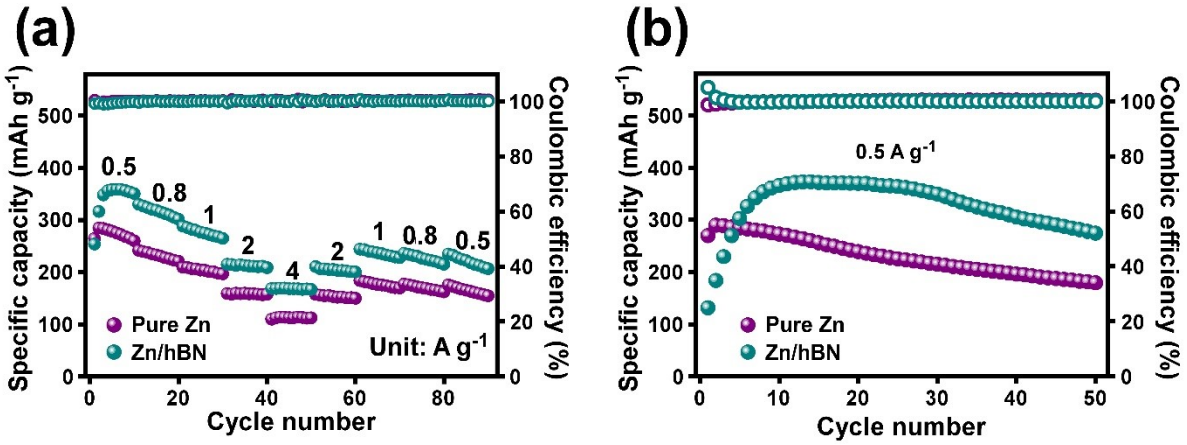

Figure S15. Electrochemical characterizations of full cell. (a) Rate performance of cell with pure Zn and Zn/hBN anodes from 0.5 to 4 A g^{-1}. (b) Cycling stability at current density of 0.5 A g^{-1}.

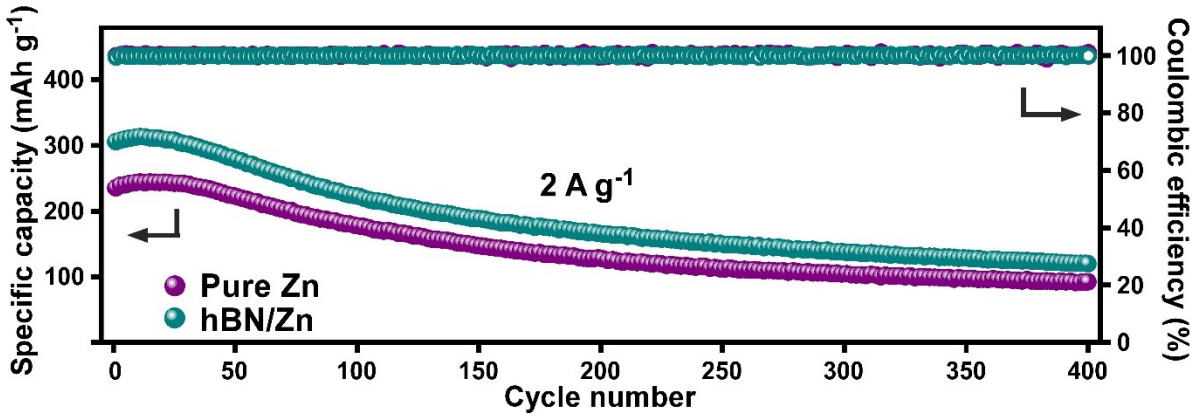

Figure S16. Electrochemical characterizations of full cell. Cycling stability at current density of 2 A g^{-1} for 400 cycles.

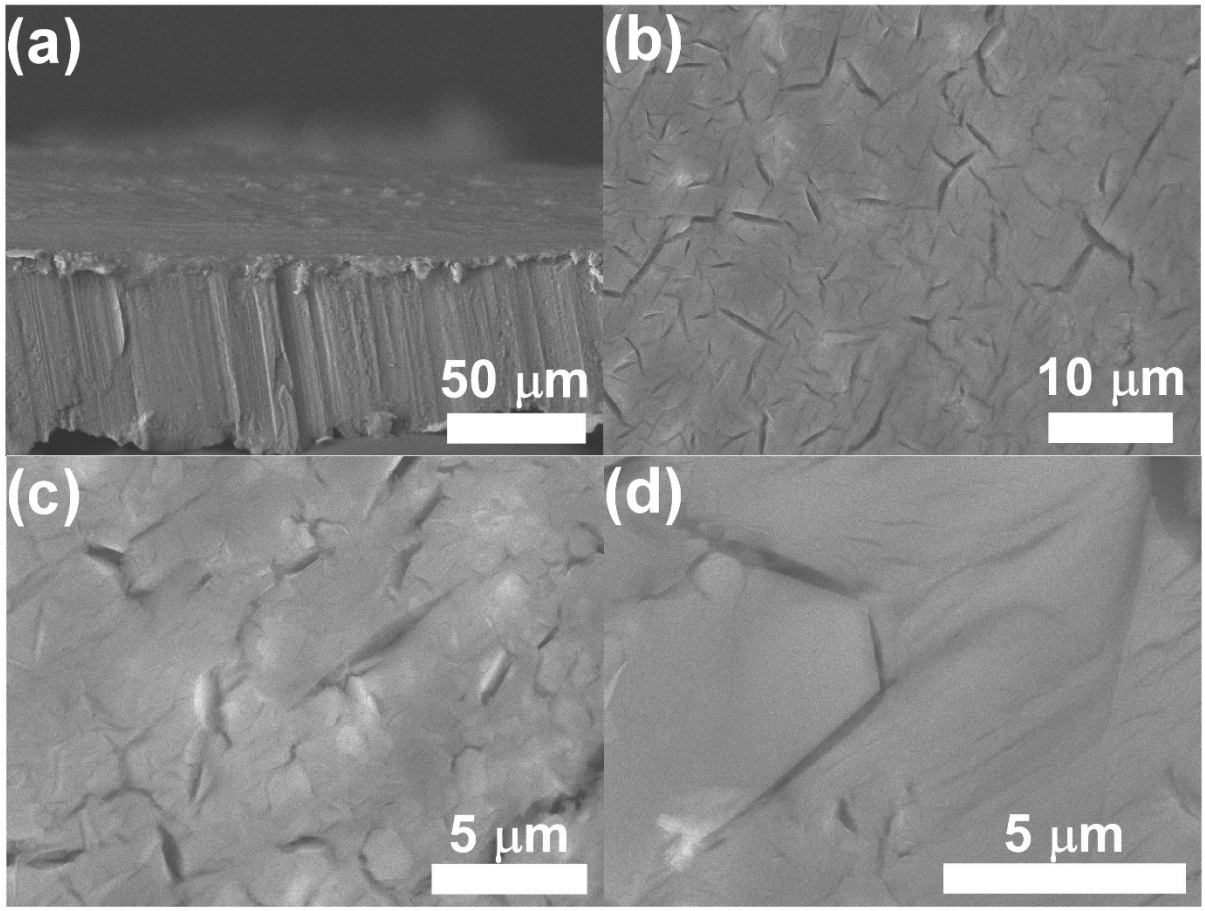

Figure S17. SEM characterization of Zn electrodeposition after 50 cycles. (a) Cross-section and (b-d) top-view of SEM images of Zn deposits after long term cycling.

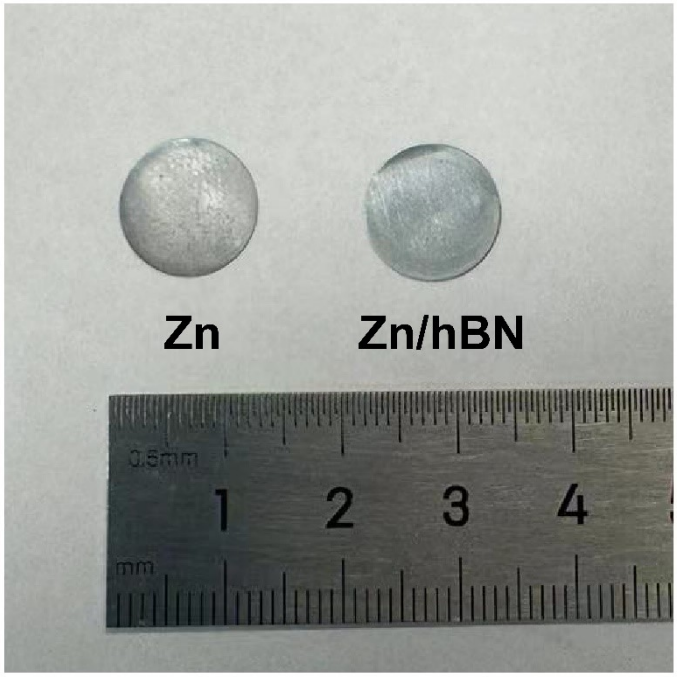

Figure S18. Optical images of Zn and Zn/hBN electrode after cycling. The color difference shows that more severe oxidation was found on Zn electrode.

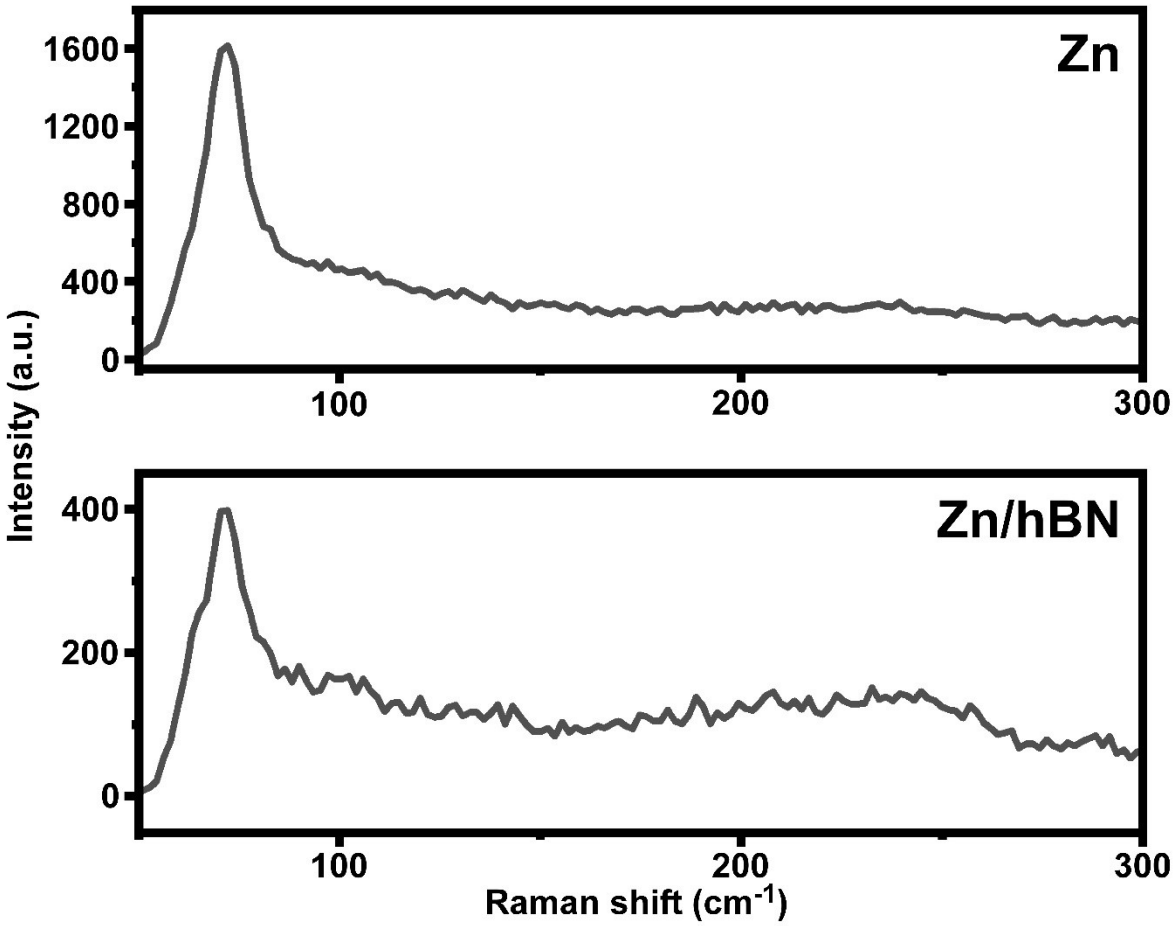

Figure S19. Raman spectrum of ZnO in the samples of Zn and Zn/hBN after cycling. The intensity comparison shows more sever Zn oxidation was found in Zn sample.

Reference

1. G. Kresse, J. F., Efficiency of ab-initio total energy calculations for metals and semiconductors using a plane-wave basis set. *Computational Materials Science* **1996,** *6*, 15-50.
2. G. Kresse, J. F., Efficient iterative schemes for ab initio total-energy calculations using a plane-wave basis set. *Physical Review B* **1996,** *54*, 11169-11186.
3. Kohn, P. H. a. W., *Physical Reivew* **1964,** *136*, B864-B871.
4. G. Kresse, D. J., From ultrasoft pseudopotentials to the projector augmented-wave method. *Physical Review B* **1999,** *59*, 1758-1775.
5. P.E.Blöchl, Projector augmented-wave method. *Physical Review B* **1994,** *50*, 17953–17979.
6. Momma, K.; Izumi, F., VESTA: a three-dimensional visualization system for electronic and structural analysis. *Journal of Applied Crystallography* **2008,** *41*, 653-658.